

Regularized Complete Cycle Consistent GAN for Anomaly Detection

Zahra Dehghanian^a, Saeed Saravani^a, Maryam Amirmazlaghani^{a,*},
Mohammad Rahmati^a

^a*Department of Computer Engineering, Amirkabir University of Technology, Iran*

Abstract

This study presents an adversarial method for anomaly detection in real-world applications, leveraging the power of generative adversarial neural networks (GANs) through cycle consistency in reconstruction error. Previous methods suffer from the high variance between class-wise accuracy which leads to not being applicable for all types of anomalies. The proposed method named RCALAD tries to solve this problem by introducing a novel discriminator to the structure, which results in a more efficient training process. Additionally, RCALAD employs a supplementary distribution in the input space to steer reconstructions toward the normal data distribution, effectively separating anomalous samples from their reconstructions and facilitating more accurate anomaly detection. To further enhance the performance of the model, two novel anomaly scores are introduced. The proposed model has been thoroughly evaluated through extensive experiments on six various datasets, yielding results that demonstrate its superiority over existing state-of-the-art models. The code is readily available to the research community at <https://github.com/zahraDehghanian97/RCALAD>.

Keywords: Anomaly detection, Generative adversarial network, Cycle consistency, Anomaly score.

^{*}Corresponding author

Email addresses: z.dehghanian@aut.ac.ir (Zahra Dehghanian), s.saravani@aut.ac.ir (Saeed Saravani), mazlaghani@aut.ac.ir (Maryam Amirmazlaghani), rahmati@aut.ac.ir (Mohammad Rahmati)

1. Introduction

Discovering dissimilar instances and rare patterns is one of the most essential tasks in real-world data. Anomaly detection is the process of finding such samples, which are known as anomalies [1]. Anomalies are an important aspect of any dataset and play an important role in a wide range of applications. For example, an irregular traffic pattern on a computer network could indicate hacking and data transmission to unauthorized places. Abnormalities in credit card transactions may reveal illicit economic activity [2], or abnormalities in an MRI image may indicate the existence of a malignant tumor [3]. Despite the existence of statistical and machine learning-based methods, designing effective models for detecting anomalies in complex, high-dimensional data spaces is still a major challenge [4].

Generative adversarial networks (GANs) have shown remarkable performance in the field of anomaly detection by overcoming this challenge and modeling the distribution of high-dimensional, complex real-world data. In GAN, a generator network is contrasted with a discriminator network; the discriminator attempts to differentiate between the real data and the data produced by the generator network. Generator and discriminator are trained simultaneously; the generator network G records the distribution of the data, and the discriminator D estimates the likelihood whether samples come from real data distribution or are being generated by G . The objective function of the generator G is to maximize the error probability of the network D . This structure leads to a two-player game like mini-max games [5].

The ability of adversarial neural networks to represent natural images has previously been demonstrated [6, 7], and their use in processing speech and text [4], as well as medical images [8] is growing. This paper proposes an efficient method for anomaly detection that is based on generative adversarial networks. Similar to many learning-based algorithms, there are two main steps: training and testing. Like other adversarial frameworks, we train the generator and discriminator networks on normal data throughout the training phase so that

both are updated in succession. In this case, the joint discriminator is used to make the training of the adversarial structure more stable. The encoder E is trained along with the discriminator and generator network to apply the inverse mapping of the input samples to the latent space. In order to find an anomalous sample, the difference between input and its reconstruction is computed and samples with high differences can be determined as anomalies.

2. Related work

Anomaly detection, also known as novelty detection and outlier detection, has been widely studied, as reviewed in [9, 10, 11]. The previous methods used in this field are generally divided into two categories: methods based on representation learning and methods based on generative models.

A representation learning method learns a mapping for the main characteristics of normal data. One-class support vector machine finds the marginal boundary around the normal data [12]. The isolation forest method is one of the classic machine learning methods. In this method, the tree is built with randomly chosen features, and the anomaly score is the average distance to the root [13]. Deep support vector data description (DSVDD) finds a hypersphere to enclose the representation of normal samples [14]. Liu and Gryllias constructed frequency domain features using cyclic spectral analysis and applied them in the support vector data description (SVDD) framework. This method has been proven robust against outliers and can achieve a high detection rate for detecting anomalies [15]. In [16], researchers presented a new approach to identify imagery anomalies by training the model on normal images altered by geometric transformation. In this model, the classifier calculates the anomaly score using softmax statistics.

Usually, generative models attempt to learn the reconstruction of the data and use this reconstruction to identify anomalous samples [17]. For instance, auto-encoders model the normal data distribution, and the reconstruction error is used as the anomaly score [18, 19]. Deep structured energy-based models

(DSEBMs) learn an energy-based model and map each sample to an energy score [20]. Deep autoencoding Gaussian mixture model (DAGMM) estimates a mixed Gaussian distribution by using an encoder for normal samples [21]. A recent line of work on anomaly detection has focused on adversarial neural networks. For example, this structure has been used to identify anomalies in medical images [8]. In this work, the inverse mapping into the latent space was performed using the recursive backpropagation mechanism. In [22], a continuation of the prior work, the mapping to the latent space was performed by the encoder in order to reduce computational complexity. In [23], the proposed model was based on bidirectional GAN (BiGAN).The encoder was also responsible for mapping the input data space to the latent space. Unlike the standard GAN structure, where the discriminator takes only the real image and the generated image of the generator network as input, the representation of these images in the latent space was also considered as input to the discriminator network. In the article [4], anomaly detection was performed by adding a new discriminator in latent space to the adversarial structure to stabilize the training process. The deep convolutional autoencoder model is a classic autoencoder model in which the encoder and decoder have a convolutional structure. The anomaly score in this model is the 2-norm of reconstruction errors [24].

In this section, we reviewed and categorized the various methods used to clarify abnormal data. In section 3 we will deep into fundamental basis required to deal with proposed model.

3. Preliminaries

In this section, we briefly elaborate the overall idea of a generative adversarial network and then concentrate on the evolution of GAN-based anomaly detection algorithms. The generative adversarial network was first proposed in 2014 by Goodfellow et al [5]. The generator and the discriminator are trained on an M set of $\{\chi^{(i)}\}_{i=1}^M$ unlabeled samples. The generator maps selected samples from the latent space z to the input data space. The discriminator attempts to distinguish

between the real data $x^{(i)}$ and the data produced by the generator (G). The generator G imitates the input data distribution, whereas the discriminator differentiates between real samples and generator data. In the training phase, the generator G and the discriminator D are alternatively optimized using a stochastic gradient descent approach.

$q(x)$ is the distribution of the input data, and $p(z)$ is the distribution of the generator in the latent space. GAN network training is done by finding a discriminator and a generator that can solve the saddle point problem as $\min_G \max_D V_{GAN}(D, G)$ and the definition of the $V_{GAN}(D, G)$ function is defined as:

$$V_{GAN} = E_{x \sim q(x)}[\log(D(x))] + E_{z \sim p(z)}[\log(1 - D(G(z)))] \quad (1)$$

Solving this problem concludes that the generator distribution is equal to the true data distribution. It has been proved in [5] that the global optimal discriminator will be obtained if and only if $p_G(x) = q(x)$. By p_G , we mean the distribution learned by the generator. Adversarially learned inference (ALI) [25] attempts to obtain the inverse mapping between input data space and latent space by modeling the joint distribution of encoder as $q(x, z) = q(x)e(z|x)$ and the distribution of generator as $p(x, z) = p(z)p(x|z)$ using the encoder E. Here, $e(z|x)$ is learned by the encoder. The objective function of the ALI model is as follows:

$$\min_{G, E} \max_D V_{ALI} = E_{q(x, z)}[\log D(x, E(x))] + E_{p(x, z)}[\log(1 - D(G(z), z))] \quad (2)$$

where D represents the discriminator, taking x and z as input, and its output value specifies probability of origination of the current inputs from the $q(x, z)$ distribution. Encoder, generator, and discriminator are in their optimal state only if $q(x, z) = p(x, z)$. This has been proved in [25].

Although p and q distributions are apparent, in practice and during model training, they are not necessarily converging to the optimal point. This issue was attributed to the problem of cycle consistency, which was defined as $G(E(x)) \approx \hat{x}$ in [26]. A new framework called ALICE was proposed to solve the above

problem by adding the discriminator D_{xx} to the ALI network structure [26].

The objective function of this model is as follows:

$$\min_{E,G} \max_{D_{xz}, D_{xx}} V_{ALICE} = V_{ALI} + E_{x \sim q(x)} [\log D_{xx}(x, x) + \log(1 - D_{xx}(x, G(E(x))))] \quad (3)$$

This work demonstrates that using a discriminator D_{xx} can achieve the best reconstruction for the input data [26]. In Adversarially Learned Anomaly Detection (ALAD), a conditional distribution was applied to the baseline ALICE model with the inclusion of additional discriminator to stabilize the training process [4]. To deep into the detail, a discriminator D_{zz} is added to the model to ensure the cycle consistency in the latent space, which tries to make the latent space variable and its reconstruction as analogous as possible. By assembling the block proposed in [4] in ALICE framework, the cost function of the ALAD model will finally be as follows:

$$\begin{aligned} & \min_{G,E} \max_{D_{xz}, D_{xx}, D_{zz}} V_{ALAD} \\ &= V_{ALICE} + \mathbb{E}_{z \sim p(z)} [\log(D_{zz}(z, z)) + \mathbb{E}_{z \sim p(z)} [\log(1 - D_{zz}(z, G(E(z))))]] \end{aligned} \quad (4)$$

In [4], it is claimed that the training model will be stabilized by adding Lipschitz constraints to the discriminators of the GAN model. Moreover, it is shown in practice that with spectral normalization of the weight parameters, the network's performance will be improved [4].

Although the idea of ALAD helps stabilize the cycle, the latent and input space variables are scrutinized in two independent spaces, and the inherent dependence between the variables is ignored. More precisely, the x and its reconstruction are investigated in a separate process from the z and its corresponding reconstruction, while the reconstruction processes of these two pairs of data is along with each other and affects each other directly. To model this reliance, we define a complete cycle and a new discriminator that employs the information contained within the complete cycle.

Another problem with ALAD is that it doesn't take into account the need for weak reconstruction for anomalous samples. In fact, in all of the previous

models, it was assumed that if the model were trained with normal data, it would always have a poor reconstruction for anomalous data, even though there is no way to force the model to make weak reconstructions of anomalous samples. The proposed RCALAD model attempts to address this issue by employing the supplementary distribution $\sigma(x)$, which biases all reconstructions toward the normal data distribution, and the model attempts to lower the anomaly score for normal input while increasing it for anomalous input.

4. Proposed Model

In this part, we describe our novel adversarial framework for anomaly detection that overcomes the aforementioned drawbacks. The problem of a lack of complete cycle consistency and our corresponding solution will be described first. Then, the necessity of weak reconstruction will be addressed. At the end of this section, two new anomaly scores based on the proposed model are introduced.

4.1. Complete Cycle Consistency

As mentioned before, in the previous models, the cycle consistency of the input data and latent space variables is examined in two independent procedures. This implies that the reconstruction of the latent space variable \hat{z} and input data \hat{x} are processed separately. It should be noted that here the variable z is a sample of the Gaussian distribution given as an input to the generator, and it is not related to the input mapping in the latent space.

The Complete Cycle Consistency issue (CCC) declares that for each variable x in the input space if the encoder first estimates the inverse mapping to the latent space, which equals $E(x) = Z_x$ and the obtained representation is entered into the generator to generate the network reconstruction from the input variable $G(Z_x) = G(E(x)) = \hat{x}$ and this reconstruction is given to the encoder network in order to calculate the reconstruction in the latent space, that is, $E(\hat{x}) = E(G(z_x)) = \hat{z}_{\hat{x}}$, it is logically expected from any reconstruction-based

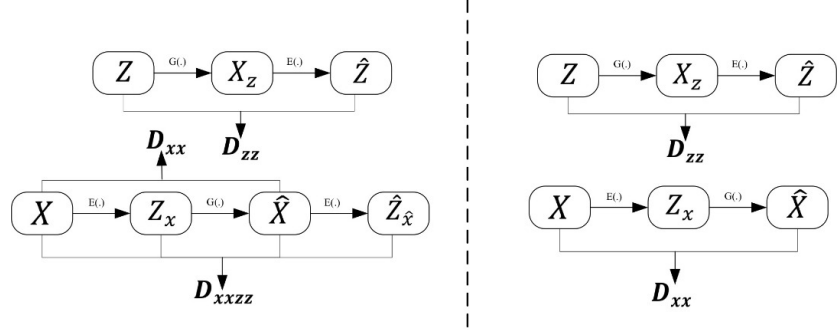


Figure 1: Using the variables of input data space and latent space in the cycle consistency of the ALAD network (right side) and the information of a complete cycle consistency in the proposed model (left side).

network that the two variables x and \hat{x} as well as the two variables \hat{z}_x and z_x have the least possible difference. That is, the CCC issue is defined in such a way that, in any reconstruction-based model, for each input sample and its mapping in the latent space, the network reconstruction for both variables should have a minimum error and maximum similarity.

Without using the CCC, the similarity between the input data and its reconstruction, as well as the similarity between z and its reconstruction, were examined independently and in two separate cycles. It was assumed that they are independent, but we know that these two cycles are entirely dependent on each other, and the assumption of independence is not valid in these two issues. To solve this problem, we proposed to model the dependency by examining the CCC variables in the new discriminator D_{xxzz} and using the information flow in this chain to improve network training for anomaly detection in the best possible way. The difference between the input of D_{xxzz} and the input of D_{zz} used in the ALAD model is represented in Figure 1.

As can be seen in Figure 1, the ALAD model does not use the information of a complete cycle. In order to use the available joint information in a complete cycle, a new variable called \hat{z}_x is introduced. To calculate this variable, the inverse mapping of the input data x is applied to the generator, and the resulting

inverse mapping is calculated again using the decoder. Hence, complete cycle consistency will be provided in this model.

In order to ensure the condition of complete cycle consistency, the new D_{xxzz} discriminator is used with the joint input. It is noteworthy that the effectiveness of the joint discriminators has already been proven once in ALIGAN [23]. Actually, when adding the encoder to the GAN framework, two procedures can be scrutinized. The first one is adding an independent discriminator to train the encoder, and the second one is changing the discriminator input from a single input mode to a joint input mode. It is proven that using a joint discriminator obtains better results. According to the same idea, the input of the joint discriminator D_{xxzz} extracts the most information for model training.

This discriminator uses the quadruple (x, x, z_x, z_x) as the real data and the quadruple of $(x, G(E(x)), z_x, E(G(z_x)))$ as the fake data. This discriminator attempts to make the input x and network reconstruction, as well as the inverse mapping of the input image in the latent space and its reconstruction by the encoder, as close as possible to each other so that a complete stable loop is provided and the model is trained and stabilized better.

4.2. Constraint of Weak Reconstruction

In reconstruction-based models, it has always been assumed that if the training and reconstruction of the normal data are properly done, the reconstruction of abnormal data will necessarily be weak and different from the input data. However, experiments indicate that it is not always the case, and sometimes the reconstructed anomalous sample is slightly similar to the input sample. Hence, it won't be easy to recognize it as an abnormal sample. In fact, in none of the previous models, there was not any obligation or control condition to bias the model toward producing poor reconstructions for anomalous samples.

During the training phase, the encoder and generator are only trained on normal samples. As a result, the appropriate z space for normal samples and the reconstruction of them is well modeled. However, because the model has not yet seen the remainder of the space, including abnormal examples, it may

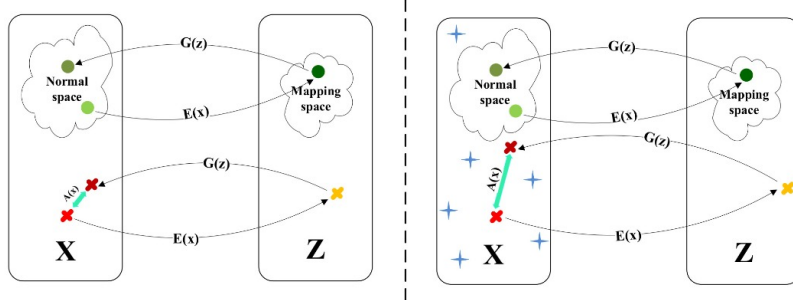


Figure 2: Effect of the presence of $\sigma(x)$ distribution in the model training process. On the right side, we have $\sigma(x)$ distribution and on the left side, there is no supplementary distribution. In this figure, x represents the input data space and z represents the latent space. Samples are mapped from the input data space to the latent space by the generator G , and the encoder E reverses the mapping. Green circles show normal samples red crosses represent abnormal samples and blue stars represent samples generated by the $\sigma(x)$ distribution. The turquoise-colored line shows the value of the abnormality score. As can be seen in Figure 1, if $\sigma(x)$ (on the left side of the figure) is not present in the training process, the abnormality score for abnormal samples is lower than when this distribution is used. On the right, the distribution of $\sigma(x)$ has biased the model towards the normal manifold.

map it onto an unknown point in the latent space during the testing phase. In this case, there is no information about mapping anomalous data to its reconstruction. To solve this problem, the supplementary distribution called $\sigma(x)$ is used. Samples from this distribution will cover the input data space, which means that we will produce some extra noisy samples and force the model to generate reconstruction in the normal data manifold. As a result, the network learns to reconstruct the normal data class for a relatively more expansive range of inputs. So an appropriate distance is created between the anomalous sample and its reconstruction. This distance is regarded as an appropriate criterion for detecting abnormal samples. Figure 2 illustrates the training routine.

4.3. RCALAD Model

In this section, we will introduce our proposed model, RCALAD, by integrating both ideas, which means employing the new variable of \hat{z}_x in the D_{xxzz} discriminator and the $\sigma(x)$ distribution and adding them to the basic model

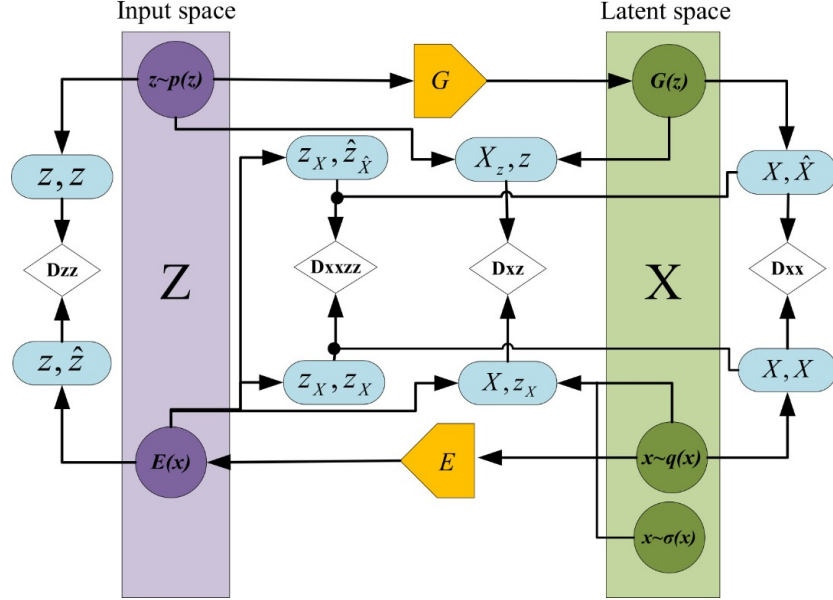


Figure 3: Overall structure of the RCALAD model.

[4]. In this network, we attempted to provide a comprehensive, practical, and compatible framework for all anomaly detection problems by resolving the aforementioned issues of the complete consistency cycle and the necessity of weak reconstruction. Figure 3 depicts a schematic representation of the proposed model. As in Figure 2, an encoder and the generator are trained in the standard structure of the adversarial neural network. The inverse mapping from the input data space to the latent space is obtained simply by using the encoder E in the proposed structure. Here, a joint discriminator called D_{xxzz} is used to train both generator and encoder networks simultaneously. This discriminator determines whether an input variable pair is derived from the input data x distribution and its corresponding point in the latent space or if it is generated by the generator G and sampled from the latent space of z . In order to satisfy the condition of cycle consistency in the input data space, D_{xx} and D_{zz} discriminators are used so cycle consistency in both latent space and input data space will be modeled independently. The D_{xxzz} is introduced to use all the information in

a complete cycle. That is, in addition to examining both variables x and z and their reconstruction in the corresponding space, their joint distribution is used in D_{xxzz} during the process of detecting anomalous samples. By using D_{xxzz} more information is available to determine whether the input data is anomalous or not. This network is responsible for determining between quadruple samples of (x, x, z_x, z_x) and $(x, G(E(x)), z_x, E(G(z_x)))$. In fact, the discriminator D_{xxzz} tries to maximize the similarity between x and its reconstruction $G(E(x))$, and it also attempts to make the mapping of the input image in the latent space z_x and its reconstruction $E(G(z_x))$ as similar as feasible. To cover much more of the latent space, the $\sigma(x)$ block is added to this model. Using this distribution, new samples are made from the input data space and then mapped into the latent space of the normal data. Finally, the objective function of the proposed model is as follows:

$$\begin{aligned} \min_{G, E} \max_{D_{xxzz}, D_{xz}, D_{xx}, D_{zz}} V_{RCALAD} (D_{xxzz}, D_{xz}, D_{xx}, D_{zz}, E, G) = \\ V_{ALAD} + E_{x \sim \sigma(x)} [\log (1 - D_{xz}(x, E(x)))] + E_{x \sim q(x)} [\log D_{xxzz}(x, x, E(x), E(x))] + \\ E_{x \sim q(x)} [1 - \log D_{xxzz}(x, G(E(x)), E(x), E(G(E(x))))] \end{aligned} \quad (5)$$

4.4. Anomaly Scores

The main goal of this proposed model is to detect anomalies based on the accurate reconstruction of normal input data, whereas abnormal samples are reconstructed in a weak manner. One of the key elements in anomaly detection is the definition of the anomaly score for calculating the distance between the input sample and the reconstruction provided by the network [4]. Some of the anomaly scores that were used in previous models are as follows:

$$\begin{aligned} A_{L_1}(x) &= \|x - \hat{x}\|_1, \\ A_{L_2}(x) &= \|x - \hat{x}\|_2, \\ A_{\text{Logits}}(x) &= \log (D_{xx}(x, \hat{x})), \\ A_{\text{Features}}(x) &= \|f_{xx}(x, x) - f_{xx}(x, \hat{x})\|_1 \end{aligned} \quad (6)$$

Here, logit means the raw output of the discriminators, while feature means the output of the layer preceding logit. In our proposed model, since the new discriminator D_{xxzz} offers the ability of extracting additional information, it is crucial to specify the new anomaly scores in order to make use of this information. Therefore, two new anomaly scores are introduced.

The first anomaly score presented in this paper is called $A_{fm}(x)$. This score uses the D_{xxzz} discriminator feature space to calculate distance between samples and their reconstruction. For this purpose, the output of the second-to-last layer is used as features. Our anomaly score is defined as follows:

$$A_{fm}(x) = \|f_{xxzz}(x, x, z_x, z_x) - f_{xxzz}(x, \hat{x}, z_x, \hat{z}_{\hat{x}})\|_1 \quad (7)$$

In this equation, $f(\cdot)$ represents the activation function of the next to last layer in the D_{xxzz} discriminator structure. The concept used in the definition of this score is using the confidence level of the discriminator on the quality of the reconstructions provided by the network. In other words, if reconstruction is performed well, the sample belongs to the trained normal data of the network. Thus, the higher value of this criterion means the greater difference in reconstructions and so higher possibility of input data's abnormality. The second point in this article is presented with the aim of maximizing the use of information in the model for anomaly detection. In this section, the A_{all} criterion is defined. The score is the sum of the outputs of all discriminators, including D_{xx} , D_{zz} and D_{xxzz} .

In fact, since all the discriminators in the proposed model are trained only based on the normal samples and the reconstruction for all the input data space is biased towards the normal data space, it is expected that the input image data and its reconstruction will look different, and the discriminators can easily identify these anomalous inputs. The mathematical expression of this criterion is given in the following equation:

$$A_{all}(x) = D_{xxzz}(x, \hat{x}, z_x, \hat{z}_{\hat{x}}) + D_{xx}(x, \hat{x}) + D_{zz}(z_x, \hat{z}_{\hat{x}}) \quad (8)$$

The criterion A_{all} tries to utilize all discriminators' information. During the

training phase, the discriminators learn to pay attention to the difference between the pairs of (x, x) and (x, \hat{x}) as well as the pairs of (z_x, z_x) and (z_x, \hat{z}_x) . It means, the farther \hat{x} from x or \hat{z}_x from z_x , it will be easier for the discriminators to recognize the data origin. In the proposed model, by adding the distribution of $\sigma(x)$ and biasing all the reconstruction towards the normal data distribution, the reconstruction error for abnormal data is increased and the discriminators' output can be considered as a reliable criterion for abnormality detection. Finally, the recommended anomaly scores can be viewed according to the algorithm 1.

Algorithm 1 Process of calculating anomaly scores in Regularized Complete Adversarially Learned Anomaly Detection

Input: $x \sim p_{x_{\text{Test}}}(x)$, E , G , D_{xx} , D_{zz} , D_{xxzz} , f_{xxzz} where f_{xxzz} is the feature layer of D_{xxzz}

Output: $A_{\text{all}}(x)$, $A_{\text{fm}}(x)$, where A is the anomaly score

procedure INFERENCE

$z_x \leftarrow E(x)$ Encode samples, Construct latent Embedding

$\hat{x} \leftarrow G(z_x)$ Reconstruct samples

$\hat{z}_x \leftarrow E(\hat{x})$ Reconstruct latent Embedding

$A_{\text{fm}}(x) \leftarrow \|f_{xxzz}(x, x, z_x, z_x) - f_{xx}(x, \hat{x}, z_x, \hat{z}_x)\|_1$

$A_{\text{all}}(x) \leftarrow D_{xxzz}(x, \hat{x}, z_x, \hat{z}_x) + D_{xx}(x, \hat{x}) + D_{zz}(z_x, \hat{z}_x)$

return $A_{\text{all}}(x), A_{\text{fm}}(x)$

end procedure

5. Experiments

This section compares the proposed RCALAD model with prominent anomaly detection models. To test the models on a fair basis, the reported outcomes for all the implemented models are based on tabular data obtained from the average of ten runs, and for each class of image data, they are based on the average of three runs. The anomaly score used in tabular data is A_{all} score and, for

image data, it is A_{fm} score. The reason for choosing these scores based on data type will be discussed later. Moreover, the ALAD model is implemented and the results of the best anomaly score A_{fm} are reported. For other models, the available results are adopted from [4, 17] .

5.1. Datasets

In order to evaluate the performance of the proposed model and scrutinize its efficiency from different viewpoints, various datasets with diverse characteristics are used. The proposed method is tested on the available image and tabular datasets. For tabular datasets, four datasets, including KDDCup99, arrhythmia, thyroid, and musk [27], are used. KDDCup99 is a dataset related to network penetration. Arrhythmia is a medical collection related to cardiac arrhythmia with 16 classes. Also, thyroid is a three-class dataset related to thyroid disease. The musk dataset was created to classify six classes of molecular musk. These four datasets, 20, 15, 2.5 and 3.2 percent of the data are anomalous samples, respectively. Hence, in the test phase, after calculating the anomaly score, the aforementioned proportion of the data that has the highest anomaly score is classified as an anomaly. In order to assess the proposed model on these datasets, F1, recall, and precision criteria are used. Two datasets, CIFAR-10 [28] and SVHN [29], are considered for the image datasets. Both of these datasets have ten classes, and, like the previous works, one class is considered as the normal class and the other nine classes as the abnormal class. The criterion used to evaluate the model on the image dataset is the area under the receiver operating curve (AUROC). For all the datasets that have been used, 80% of the data were used for training, and 20% were used for testing. Validation data is chosen from 25% of the training data. It is noteworthy that, in the training phase, all the anomalous samples are eliminated from the training data.

5.2. Experiments on the Tabular Datasets

Evaluation results of the proposed RCALAD model and other state-of-the-art models on tabular datasets (KDDCup99, arrhythmia, thyroid, and musk)

are summarized in Table 1. The structures used in the generator, discriminator, and encoder networks are all fully connected layers with nonlinear activation functions. It should be noted that, in this step, $N(0, I)$ distribution is used as $\sigma(x)$. In comparison to existing models, the proposed model has a successful performance on the arrhythmia and musk datasets, as shown in Table 1. Our model is also the best according to F1 criteria on the KDD dataset, but it takes second place on the thyroid dataset due to the exceptional performance of the IF model. The reason for this phenomenon can be attributed to the nature of the data in this dataset. Since there are various features in this dataset, only a few of them are informative; therefore, the results of classic models such as IF, which are based on feature selection, are better. An idea to improve the proposed model results on the thyroid dataset is to use models such as IF in the preprocessing step to select more informative features for training the model.

Table 1: Output results of the proposed model in comparison with the basic models on the tabular data set.

Model	KDDCup			Arrhythmia			Thyroid			Musk		
	Prec.	Recall	F1 score									
IF[25]	92.1	93.7	92.9	51.4	54.6	53.0	70.1	71.4	70.2	47.9	47.7	47.5
OC-SVM[12]	74.5	85.2	79.5	53.9	40.8	45.1	36.3	42.3	38.8	—	—	—
DSEBMr[20]	85.1	64.7	73.2	15.1	15.1	15.1	4.0	4.03	4.0	—	—	—
DSEBMe[20]	86.1	64.4	73.9	46.6	45.6	46.0	13.1	13.1	13.1	—	—	—
AnoGAN[8]	87.8	82.9	88.6	41.1	43.7	42.4	44.1	46.8	45.4	3.0	3.1	3.1
DAGMM[26]	92.9	94.2	93.6	49.0	50.7	49.8	47.6	48.3	47.8	—	—	—
ALAD[4]	94.2	95.7	95.0	50.0	53.1	51.5	22.9	21.5	22.2	58.1	59.0	58.3
DSVDD[13]	89.8	94.9	92.1	35.3	34.3	34.7	22.2	23.6	23.2	—	—	—
RCALAD	95.3	95.6	95.4	58.8	62.5	60.6	53.7	51.5	52.6	62.9	63.3	63.1

5.3. Experiments on the image Datasets

In this section, the performance of the proposed model on CIFAR-10 and SVHN image data is scrutinized in two separate tables. All the experiment are done in one vs. all setting.

As in Tables 2 and 3, the proposed model has significantly improved the results on the CIFAR-10 dataset. The results show that the model performs

best in the half of classes and gets competitive results on others. In addition to being superior in seven classes on SVHN dataset, the proposed model also performs the best in the average of all classes. Furthermore our model decreases class-wise variance on image datasets that leads to more reliable results. We provide some example of input images with their reconstruction in 4 and 5. As you can see our model produces reconstructions in normal data manifold even for anomalous samples. For example the proposed model can reconstructs a dog image as a car.

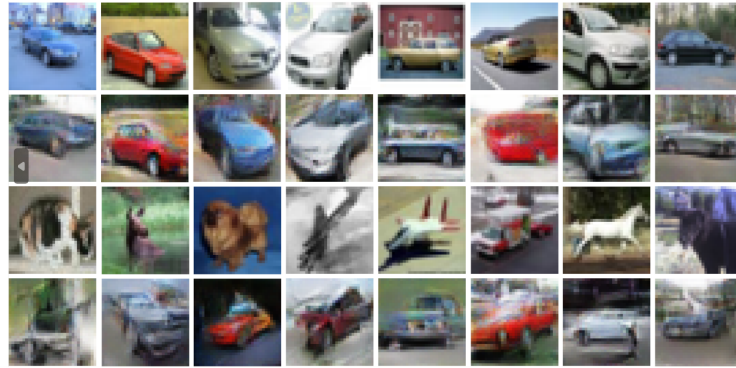


Figure 4: Reconstruction of normal and abnormal inputs on CIFAR-10 dataset. The first row is normal inputs and the second row is their reconstruction. The third row are anomalies and the fourth row is corresponding reconstruction for anomalies.

5.4. Ablation Studies

In this section, we examine the effectiveness of each component added to the basic model on both kinds of datasets. In these experiments, the average results of the model are repeated in the presence and absence of the discriminator D_{xxzz} and the supplementary distribution $\sigma(x)$.

According to Tables 4 and 5, the proposed RCALAD model achieves the best result in the presence of both parts. In scrutinizing the role of the D_{xxzz} discriminator, this discriminator has improved the accuracy on the CIFAR-10 dataset to an optimal level but has not made significant improvement on the SVHN dataset. In terms of the role of the $\sigma(x)$ distribution, it performed well



Figure 5: Reconstruction of normal and abnormal inputs on SVHN dataset. The first row is normal inputs and the second row is their reconstruction. The third row are anomalies and the fourth row is corresponding reconstruction for anomalies.

Table 2: Output results of the proposed model compared to the basic models on the CIFAR-10 dataset.

Normal	DCAE[30]	DSEBM[20]	DAGMM[26]	IF[25]	AnoGAN[8]	ALAD[4]	RCALAD
Airplane	59.1	41.4	56.0	60.1	67.1	64.7	68.4
car	57.4	57.1	56.0	50.8	54.7	45.7	57.2
Bird	48.9	61.9	53.8	49.2	52.9	67.0	69.6
Cat	58.4	50.1	51.2	55.1	54.5	59.2	67.2
Deer	54.0	73.2	52.2	49.8	65.1	72.7	71.9
Dog	62.2	60.5	49.3	58.5	60.3	52.8	65.1
Frog	51.2	68.4	64.9	42.9	58.5	69.5	70.3
Horse	58.6	53.3	55.3	55.1	62.5	44.8	59.6
Ship	76.8	73.9	51.9	74.2	75.8	73.4	70.5
Truck	67.3	63.6	54.2	58.9	66.5	43.2	57.6
Mean	59.4	60.3	54.4	55.5	61.8	59.3	65.7

on the CIFAR-10 dataset and enhanced the AUROC criterion. However, when applied to the SVHN dataset, it reduced the AUROC criteria by a tiny amount when compared to the base model. Still, its inclusion in the final model resulted in the extraction of new information and a more comprehensive view.

Table 3: Output results of the proposed model compared to the basic models on the SVHN dataset.

Normal	OCSVM[12]	DSEBMr[20]	DSEBMe[20]	IF[25]	AnoGAN[8]	ALAD[4]	RCALAD
0	52.0	56.1	53.4	53.0	57.3	58.7	60.4
1	48.6	52.3	52.1	51.2	57.0	62.8	59.2
2	49.7	51.9	51.8	52.3	53.1	55.2	54.9
3	50.9	51.8	51.7	52.2	52.6	53.8	55.8
4	48.4	52.5	52.4	49.1	53.9	58.0	58.5
5	51.1	52.4	52.3	52.4	52.8	56.1	56.2
6	50.1	52.1	52.2	51.8	53.2	57.4	59.4
7	49.6	53.4	55.3	52.0	55.0	58.8	58.0
8	45.0	51.9	52.5	52.3	52.2	55.2	56.1
9	52.5	55.8	52.7	53.7	53.1	57.3	58.3
Mean	50.2	52.9	52.4	51.6	54.0	57.3	57.7

Table 4: Effects of the various proposed sections in improving the results of the image datasets.

Model	AUROC
CIFAR-10	
Baseline(ALAD)	59.3
Baseline + D_{xxzz} (CALAD)	63.4
Baseline + $\sigma(x)$ (RALAD)	64.2
Baseline + $D_{xxzz} + \sigma(x)$ (RCALAD)	65.7
SVHN	
Baseline(ALAD)	57.3
Baseline + D_{xxzz} (CALAD)	57.6
Baseline + $\sigma(x)$ (RALAD)	56.8
Baseline + $D_{xxzz} + \sigma(x)$ (RCALAD)	57.7

5.5. Evaluating the Sufficiency of the D_{xxzz}

By adding the D_{xxzz} discriminator, is there a need for D_{xx} and D_{zz} discriminators or not? To answer this question correctly, we performed some experiments, whose results are summarized in Table 6. In fact, in this section, in

Table 5: Effects of the various proposed sections in improving the results of the tabular datasets.

Model	Precision	Recall	F1 score
KDDCup99			
Baseline(ALAD)	94.4	95.7	95.0
Baseline + D_{xxzz} (CALAD)	95.9	95.7	95.8
Baseline + $\sigma(x)$ (RALAD)	94.3	95.5	94.9
Baseline + $D_{xxzz} + \sigma(x)$ (RCALAD)	95.3	95.6	95.4
Arrhythmia			
Baseline(ALAD)	50.0	53.1	51.5
Baseline + D_{xxzz} (CALAD)	57.4	60.5	57.5
Baseline + $\sigma(x)$ (RALAD)	54.6	56.5	55.5
Baseline + $D_{xxzz} + \sigma(x)$ (RCALAD)	58.8	62.5	60.6
Thyroid			
Baseline(ALAD)	22.9	21.5	22.2
Baseline + D_{xxzz} (CALAD)	52.9	51.8	52.3
Baseline + $\sigma(x)$ (RALAD)	43.1	45.7	44.3
Baseline + $D_{xxzz} + \sigma(x)$ (RCALAD)	53.7	51.5	52.6
Musk			
Baseline(ALAD)	50.0	53.1	51.5
Baseline + D_{xxzz} (CALAD)	57.4	60.5	57.5
Baseline + $\sigma(x)$ (RALAD)	54.6	56.5	55.5
Baseline + $D_{xxzz} + \sigma(x)$ (RCALAD)	62.9	63.3	63.1

addition to the above-mentioned question, the result of adding D_{xxzz} discriminator in basic models such as ALI and ALICE are investigated.

In Table 6 we examine the effects of all discriminators on different models. According to this table and as expected from the theoretical results, adding the D_{xxzz} discriminator to the general frameworks had the highest efficiency. As a result, eliminating D_{xx} has less of an impact on the model because some of the information it collects is covered by the D_{xxzz} discriminator. However, it is apparent that removing D_{zz} , which assesses the similarity of z and its reconstruction in an independent cycle, decreases the accuracy. As can be seen, employing these three discriminators is seen to be the most effective, as the

D_{xxzz} discriminator alone does not cover all aspects. It is worth noting that this remark applies to both image and tabular datasets.

Table 6: Assessing the performance of the model in the presence or absence of each of the discriminators.

model	D_{zz}	D_{xx}	D_{xxzz}	Precision	Recall	F1 score
KDDCup99						
ALAD	yes	yes	no	94.2	95.7	95.0
ALI + D_{xxzz}	no	no	yes	93.8	95.1	94.4
ALI + $D_{zz} + D_{xxzz}$	yes	no	yes	94.6	95.5	95.0
ALICE + D_{xxzz}	no	yes	yes	94.1	94.5	94.7
CALAD	yes	yes	yes	95.9	95.7	95.8
RCALAD	yes	yes	yes	95.3	95.6	95.4
Arrhythmia						
ALAD	yes	yes	no	50.0	53.1	51.5
ALI + D_{xxzz}	no	no	yes	52.2	52.9	52.5
ALI + $D_{zz} + D_{xxzz}$	yes	no	yes	57.1	58.2	57.6
ALICE + D_{xxzz}	no	yes	yes	54.3	56.1	55.1
CALAD	yes	yes	yes	57.4	60.5	57.5
RCALAD	yes	yes	yes	58.8	62.5	60.6

5.6. Scores Evaluation

In this section, the proposed anomaly scores are evaluated and compared with the anomaly scores presented in previous work [4]. As shown in Table 7, on tabular data, the raw output of the D_{xxzz} discriminator A_{all} outperforms other anomaly scores. The performance of the feature-based score A_{fm} on image data is remarkable, as can be seen in Table 8. This difference in the performance of the introduced scores can be attributed to the difference in the number of features in these two types of datasets. Given the fact that the number of features on tabular data is less than those on image data, the outputs of all discriminators are enough to detect anomalous data. However, in the image datasets, the output of the next-to-last layer contains more information

Table 7: Comparing the performance of the proposed anomaly scores with other scores on tabular data

Score	Precision	Recall	F1 score
KDDCup99			
A_{L_1}	90.8	91.0	90.9
A_{L_2}	90.1	90.0	90.0
A_{Logits}	91.6	91.6	91.6
$A_{Features}$	91.2	91.7	91.1
A_{fm}	93.2	93.7	93.0
A_{all}	92.3	90.0	92.1
Arrhythmia			
A_{L_1}	35.2	37.5	36.4
A_{L_2}	35.2	37.5	36.4
A_{Logits}	55.8	59.3	57.6
$A_{Features}$	23.2	25.0	24.2
A_{fm}	44.1	46.8	45.4
A_{all}	61.7	65.6	63.7
Thyroid			
A_{L_1}	49.8	49.0	49.9
A_{L_2}	50.1	50.0	50.0
A_{Logits}	49.6	49.7	49.7
$A_{Features}$	51.2	51.7	51.5
A_{fm}	52.2	51.2	51.7
A_{all}	53.7	51.5	52.6
Musk			
A_{L_1}	59.7	59.3	59.5
A_{L_2}	60.0	60.1	60.1
A_{Logits}	58.6	58.9	58.8
$A_{Features}$	58.2	58.8	58.8
A_{fm}	61.1	61.8	61.4
A_{all}	62.9	63.3	63.1

to distinguish between normal and abnormal data. In this way, the A_{fm} score excelled on the image datasets, while A_{all} performed well on tabular datasets.

Table 8: Comparing the performance of the proposed anomaly scores with other scores on image datasets.

Anomaly Score	AUROC
CIFAR-10	
A_{L_1}	63.4
A_{L_2}	63.2
A_{Logits}	62.9
$A_{Features}$	63.1
A_{fm}	65.7
A_{all}	64.7
SVHN	
A_{L_1}	57.7
A_{L_2}	56.3
A_{Logits}	53.6
$A_{Features}$	57.6
A_{fm}	57.7
A_{all}	57.6

6. Conclusion

This research presents a unique and cutting-edge solution for anomaly detection through the use of generative adversarial neural networks (GANs). The proposed framework utilizes an encoder to invert the mapping of the input data space and incorporates two discriminators, D_{xx} and D_{zz} , to improve the stability of the training process and ensure a consistent cycle. To further enhance the information utilization of the cycle, a new discriminator, D_{xxzz} , is introduced. The model also incorporates a supplementary distribution $\sigma(x)$ to influence the network output to align with the normal data distribution, leading to even more precise anomaly detection. The results of the experiments are truly remarkable, with the proposed model outperforming existing state-of-the-art models for both

tabular and image datasets in terms of anomaly detection and reducing class-wise variance in image datasets. Although the RCALAD model faces the same robustness challenges as other GAN-based models, these issues can be addressed through existing methods as described in [31, 32].

References

- [1] D. Yao, X. Shu, L. Cheng, S. J. Stolfo, Anomaly detection as a service: challenges, advances, and opportunities, *Synthesis Lectures on Information Security, Privacy, and Trust* 9 (3) (2017) 1–173.
- [2] C. Jiang, J. Song, G. Liu, L. Zheng, W. Luan, Credit card fraud detection: A novel approach using aggregation strategy and feedback mechanism, *IEEE Internet of Things Journal* 5 (5) (2018) 3637–3647.
- [3] X. Dai, M. Bikdash, Distance-based outliers method for detecting disease outbreaks using social media, in: *SoutheastCon 2016*, IEEE, 2016, pp. 1–8.
- [4] H. Zenati, M. Romain, C.-S. Foo, B. Lecouat, V. Chandrasekhar, Adversarially learned anomaly detection, in: *2018 IEEE International conference on data mining (ICDM)*, IEEE, 2018, pp. 727–736.
- [5] I. Goodfellow, J. Pouget-Abadie, M. Mirza, B. Xu, D. Warde-Farley, S. Ozair, A. Courville, Y. Bengio, Generative adversarial nets, *Advances in neural information processing systems* 27 (2014).
- [6] A. Radford, L. Metz, S. Chintala, Unsupervised representation learning with deep convolutional generative adversarial networks, *arXiv preprint arXiv:1511.06434* (2015).
- [7] A. Creswell, T. White, V. Dumoulin, K. Arulkumaran, B. Sengupta, A. A. Bharath, Generative adversarial networks: An overview, *IEEE signal processing magazine* 35 (1) (2018) 53–65.
- [8] T. Schlegl, P. Seeböck, S. M. Waldstein, U. Schmidt-Erfurth, G. Langs, Unsupervised anomaly detection with generative adversarial networks to guide

marker discovery, in: International conference on information processing in medical imaging, Springer, 2017, pp. 146–157.

- [9] R. Kaur, S. Singh, A survey of data mining and social network analysis based anomaly detection techniques, *Egyptian informatics journal* 17 (2) (2016) 199–216.
- [10] A. Zimek, E. Schubert, H.-P. Kriegel, A survey on unsupervised outlier detection in high-dimensional numerical data, *Statistical Analysis and Data Mining: The ASA Data Science Journal* 5 (5) (2012) 363–387.
- [11] M. A. Pimentel, D. A. Clifton, L. Clifton, L. Tarassenko, A review of novelty detection, *Signal processing* 99 (2014) 215–249.
- [12] B. Schölkopf, R. C. Williamson, A. Smola, J. Shawe-Taylor, J. Platt, Support vector method for novelty detection, *Advances in neural information processing systems* 12 (1999).
- [13] L. Ruff, R. Vandermeulen, N. Goernitz, L. Deecke, S. A. Siddiqui, A. Binder, E. Müller, M. Kloft, Deep one-class classification, in: International conference on machine learning, PMLR, 2018, pp. 4393–4402.
- [14] S. Liang, Y. Li, R. Srikant, Enhancing the reliability of out-of-distribution image detection in neural networks, *arXiv preprint arXiv:1706.02690* (2017).
- [15] C. Liu, K. Gryllias, A semi-supervised support vector data description-based fault detection method for rolling element bearings based on cyclic spectral analysis, *Mechanical Systems and Signal Processing* 140 (2020) 106682.
- [16] I. Golan, R. El-Yaniv, Deep anomaly detection using geometric transformations, *Advances in neural information processing systems* 31 (2018).
- [17] Z. Yang, I. S. Bozchalooi, E. Darve, Regularized cycle consistent generative adversarial network for anomaly detection, *arXiv preprint arXiv:2001.06591* (2020).

- [18] D. T. Nguyen, Z. Lou, M. Klar, T. Brox, Anomaly detection with multiple-hypotheses predictions, in: International Conference on Machine Learning, PMLR, 2019, pp. 4800–4809.
- [19] S. Pidhorskyi, R. Almohsen, G. Doretto, Generative probabilistic novelty detection with adversarial autoencoders, *Advances in neural information processing systems* 31 (2018).
- [20] S. Zhai, Y. Cheng, W. Lu, Z. Zhang, Deep structured energy based models for anomaly detection, in: International conference on machine learning, PMLR, 2016, pp. 1100–1109.
- [21] T. Schlegl, P. Seeböck, S. M. Waldstein, G. Langs, U. Schmidt-Erfurth, f-anogan: Fast unsupervised anomaly detection with generative adversarial networks, *Medical image analysis* 54 (2019) 30–44.
- [22] H. Zenati, C. S. Foo, B. Lecouat, G. Manek, V. R. Chandrasekhar, Efficient gan-based anomaly detection, *arXiv preprint arXiv:1802.06222* (2018).
- [23] V. Dumoulin, I. Belghazi, B. Poole, O. Mastropietro, A. Lamb, M. Arjovsky, A. Courville, Adversarially learned inference, *arXiv preprint arXiv:1606.00704* (2016).
- [24] C. Li, H. Liu, C. Chen, Y. Pu, L. Chen, R. Henao, L. Carin, Alice: Towards understanding adversarial learning for joint distribution matching, *Advances in neural information processing systems* 30 (2017).
- [25] F. T. Liu, K. M. Ting, Z.-H. Zhou, Isolation forest, in: 2008 eighth ieee international conference on data mining, IEEE, 2008, pp. 413–422.
- [26] B. Zong, Q. Song, M. R. Min, W. Cheng, C. Lumezanu, D. Cho, H. Chen, Deep autoencoding gaussian mixture model for unsupervised anomaly detection, in: International conference on learning representations, 2018.
- [27] D. Dua, C. Graff, UCI machine learning repository (2017).
URL <http://archive.ics.uci.edu/ml>

- [28] A. Krizhevsky, G. Hinton, et al., Learning multiple layers of features from tiny images (2009).
- [29] Y. Netzer, T. Wang, A. Coates, A. Bissacco, B. Wu, A. Y. Ng, Reading digits in natural images with unsupervised feature learning, in: NIPS Workshop on Deep Learning and Unsupervised Feature Learning 2011, 2011.
URL http://ufldl.stanford.edu/housenumbers/nips2011_housenumbers.pdf
- [30] A. Makhzani, B. J. Frey, Winner-take-all autoencoders, *Advances in neural information processing systems* 28 (2015).
- [31] T. Salimans, I. Goodfellow, W. Zaremba, V. Cheung, A. Radford, X. Chen, Improved techniques for training gans, *Advances in neural information processing systems* 29 (2016).
- [32] R. Chalapathy, A. K. Menon, S. Chawla, Robust, deep and inductive anomaly detection, in: *Joint European Conference on Machine Learning and Knowledge Discovery in Databases*, Springer, 2017, pp. 36–51.